Water Science and Engineering 2020, 13(1): 57−64

HOSTED BY

ELSEVIER

Available online at www.sciencedirect.com

Water Science and Engineering

journal homepage: wse.hhu.edu.cn

Ecological impact of land reclamation on Jiangsu coast (China): A novel ecotope assessment for Tongzhou Bay

Jos R.M. Muller [a,b,*], Yong-ping Chen [c], Stefan G.J. Aarninkhof [a], Ying-Chi Chan [d,e], Theunis Piersma [d,e], Dirk S. van Maren [a,f], Jian-feng Tao [c], Zheng Bing Wang [a,f], Zheng Gong [c]

[a] *Faculty of Civil Engineering and Geosciences, Delft University of Technology, Delft 2600 GA, the Netherlands*
[b] *Baggermaatschappij Boskalis BV, Papendrecht 3350 AE, the Netherlands*
[c] *College of Harbor, Coastal and Offshore Engineering, Hohai University, Nanjing 210098, China*
[d] *Groningen Institute for Evolutionary Life Sciences (GELIFES), University of Groningen, Groningen 9700 CC, the Netherlands*
[e] *Department of Coastal Systems, NIOZ Royal Netherlands Institute for Sea Research and Utrecht University, Den Burg 1790 AB, the Netherlands*
[f] *Unit of Marine and Coastal Systems, Deltares, Delft 2600 MH, the Netherlands*

Received 1 August 2019; accepted 27 November 2019
Available online 4 April 2020

Abstract

China's continuous and rapid economic growth has led to the reclamation of large sections of the intertidal mud coast in combination with port construction, such as that of the proposed Tongzhou Bay port on the Jiangsu coast. These reclamations threaten the local ecosystem services. An ecotope distribution map was created and a hydrodynamic numerical model of Tongzhou Bay was set up to quantify the impacts of reclamation on the ecosystem. Based on the field data and model results, several abiotic features were classified into 11 ecotopes and visualized in an ecotope map of the Tongzhou Bay ecosystem. Validation with spatial distributions of two threatened shorebird species (bar-tailed godwit and great knot) showed confirmation with the mid-range and low-range littoral zones (inundated from 40% to 100% of a tidal cycle), indicating the importance of the areas with these conditions to these populations. Overlaying the ecotope map with recent and proposed land reclamation schemes revealed a loss of ecotopes, composed of the high-range (42%), mid-range (48%), and low-range (38%) littoral habitats, corresponding to a 44%−45% loss of the most important ecotopes for bar-tailed godwit and great knot (mid-range and low-range littoral zones). These results confirm the applicability of the novel ecotope assessment approach in practice.

Keywords: Mapping; Ecotope; Ecotope map; Intertidal mudflats; Migratory shorebirds; Reclamation; Tongzhou Bay; Jiangsu coast

1. Introduction

Over the last few decades, China has experienced immense economic development, during which the Chinese central government has promoted the urbanization and industrial development of coastal provinces by reclaiming large sections of coastal zones (Ma et al., 2014; Tian et al., 2016). A salient contemporary case is Tongzhou Bay on the Jiangsu coast (Fig. 1). This area is characterized by large intertidal mudflats (e.g., Yaosha and Lengjiasha) with deep tidal channels (e.g., Xiaomiaohong and Sanshahong) and has a high potential for the development of agri-aquaculture, as well as the construction of the new deep-sea Tongzhou Bay port (Wang and Wall, 2010; Zhang and Chen, 2011). Recently, a new masterplan for the development of the Tongzhou Bay port before 2035 has been announced, proposing the reclamation of large sections of the Yaosha shoal (Nantong Leju Network, 2019).

This work was supported by the National Key Research and Development Program of China (Grant No. 2017YFC0405401) and the Science and Technology Project of Traffic and Transportation in Jiangsu Province (Grant No. 2017ZX01).

* Corresponding author.
E-mail address: jos.muller@boskalis.com (Jos R.M. Muller).

Peer review under responsibility of Hohai University.

https://doi.org/10.1016/j.wse.2020.04.001

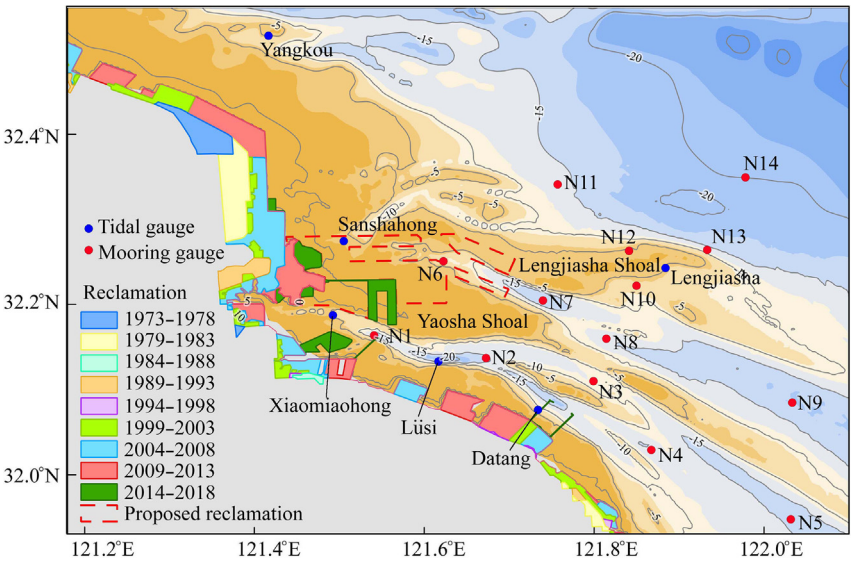

Fig. 1. Overview of shoals and channels in Tongzhou Bay situated at southern Jiangsu coast (units of elevations: m).

However, the Yellow Sea coastal wetlands form an essential part of the East Asian-Australasian Flyway (Murray et al., 2015). Reclamation activities including those at the Jiangsu coast have shown to be linked to the decline of wetland ecosystem and endangered shorebird species (Murray et al., 2014, 2015; Piersma et al., 2016). The proposed Tongzhou Bay port would strongly interfere with the habitat required by migratory shorebirds. Previous modeling efforts have provided a better understanding of the complex hydro- and morphodynamics at Tongzhou Bay (Wang et al., 2012; Xing et al., 2012; Xu et al., 2016; Yao, 2016) and the impacts of reclamation activities on these processes (Huang and Liu, 2017; Tao et al., 2011; Zhang et al., 2013). However, little is known about the consequences for the wetland habitat. Hydrodynamic conditions are a main determinant of spatial distribution of tidal wetland organisms, such as marsh vegetation (Wu et al., 2017), and ecotope distribution maps are a useful approach to assessing the impact of reclamation activities on Tongzhou Bay on potential habitat zones. These ecotope maps describe the relationship between the abiotic system and biotic elements and are often used as a tool in determining habitat maintenance and development policies (Bouma et al., 2005).

In this study we integrated a hydrodynamic model and unique distributional data of two of the main species of shorebirds, the bar-tailed godwit (*Limosa lapponica*, BTG) and great knot (*Calidris tenuirostris*, GK) in the Tongzhou Bay wetlands. First, we developed a hydrodynamic numerical model for the Tongzhou Bay region based on a large-scale model for the entire Jiangsu coast (Su, 2016; Yao, 2016). The validated model was then used to quantify ecosystem distribution at Tongzhou Bay for the 2012 situation, which was then compared with the distributional data of the shorebirds. Finally, the current reclamation (from 2014 to 2018) and proposed reclamation (from 2019 to 2035) were overlaid on the ecotope distribution to assess their combined impact.

2. Methodology

2.1. Ecotope classification

Ecotopes in the Tongzhou Bay system were quantified with the ZES.1 method (Bouma et al., 2005) that was developed for saline open water ecosystems in the Netherlands, and also applied to the entire Wadden Sea (Baptist et al., 2019). It was assumed that the ZES.1 salt water classification method was also applicable to the Jiangsu coast. An ecotope only describes a potential niche for the possible occurrence of a certain habitat and validation of the findings is therefore required. Regions with relatively homogeneous habitat characteristics can be determined, by selecting relevant abiotic features that dictate the occurrence of certain habitats in a hierarchical manner and defining class boundaries.

Field data were available for this analysis, including salinity, water level, bathymetry, and current velocities (CCCC Third Harbor Consultants Co., Ltd., 2012; Yao, 2016). Hence, the ecotope classification was based on the salinity, substrate, water depth, flow velocity, and dryfall period (e.g., the period when the mudflats are not inundated during a tidal cycle) for the situation corresponding to 2012. Since the hydrodynamic data were only measured at several locations, a well-validated hydrodynamic model (Section 2.3) was refined and validated for the Tongzhou Bay region to generate the high-resolution spatial hydrodynamic data needed for ecotope mapping. The tidal system is driven by two large-scale rotary tidal currents in the Bohai, Yellow, and East China seas (BYECS), that converge at Jianggang, creating a “rope-skipping” pattern (Xing et al., 2012; Kang et al., 2015). The local hydrodynamic setting is dominated by a semi-diurnal tide, with a consequent tidal range of 3.9 m at Lüsi Station (Su et al., 2015; Kang et al., 2015). To retrieve the average water depth, tidal current, and dryfall period, two consecutive tidal cycles were simulated.

The definition of the class bounds followed the method described by Bouma et al. (2005). Data analysis revealed small variations in salinity, as well as a homogenous soft substrate over the Tongzhou Bay region, which was considered constant. Depth classification was based on the tidal datum (e.g., mean high water neaps (*MHWN*) and mean low water springs (*MLWS*)), consistent with Bouma et al. (2005). In this study, the classification of high hydrodynamic and low hydrodynamic features was based on the maximum linear velocity of 0.8 m/s. This value was derived from the initiation of bed forms, which implies a change in bed level and ecotope distribution as found for the Wadden Sea (Baptist et al., 2016; Bouma et al., 2005). Further classification based on bed soil composition was not included, due to the lack of high-resolution soil data and the smaller impact that would have on habitat occurrence. However, low flow velocities often correspond to silt-rich bed soils. Classification based on the dryfall period was consistent with the ZES.1 method. However, a lower limit of high-range littoral zone of 60% of a tidal cycle was chosen to match the field observations. A color scheme was assigned to each defined ecotope to set up an ecotope distribution map, and the features and names of the ecotopes are shown in Table 1.

2.2. Bird satellite tracking analysis

To verify the ecotope map, satellite-tracking data of two migratory shorebird species, BTG and GK, were used. They are two of the main species using wetlands of the Jiangsu coast (Peng et al., 2017; Piersma et al., 2017) as an important fueling stop during their spring and autumn migration (Battley et al., 2012; Chan et al., 2019b; Piersma et al., 2017). Under the 1999 Environment Protection and Biodiversity Conservation Act of the Australian government, both BTG (the *menzbieri* subspecies being tracked in this study) and GK are listed as *critically endangered* (Australian Government, 2019). Solar platform terminal transmitters (PTTs, Microwave Telemetry, USA) of 4.5 g and 9.5 g were deployed onto individual birds in Roebuck Bay, Broome (17.98°S, 122.31°E) and Eighty Mile Beach (19.40°S, 121.27°E), Northwest Australia. These transmitters send signals to Argos satellites, from which the birds' locations were estimated (for details see Chan et al. (2019b)). For each species, we estimated kernel density home ranges from all locations collected on the Jiangsu coast from April 2015 to September 2017. Kernel density contours were calculated to show the areas where these species generally occurred (90% and 95% home ranges), and the core (intensively used) areas (50%).

2.3. Numerical model and model setup

The hydrodynamics at Tongzhou Bay were calculated with the Delft3D numerical model (Lesser et al., 2004). In order to accurately predict the tidal flow, the model consisted of an online coupled domain of Tongzhou Bay within a stand-alone model of the Jiangsu coast (Fig. 2). The Jiangsu regional model (JRM) encompasses the entire Jiangsu coast, with boundaries from north of the Yangtze River mouth to the Shandong Peninsula (Su, 2016; Yao, 2016). The JRM used a computational grid of 573 × 346 grid cells with a resolution varying from 600 to 1200 m. The Tongzhou Bay model (TBM) covered the Yaosha-Lengjiasha ridge as well as the more nearshore areas of Lüsi and Rudong. The computational grid consisted of 269 × 468 cells with a resolution varying from 300 to 400 m.

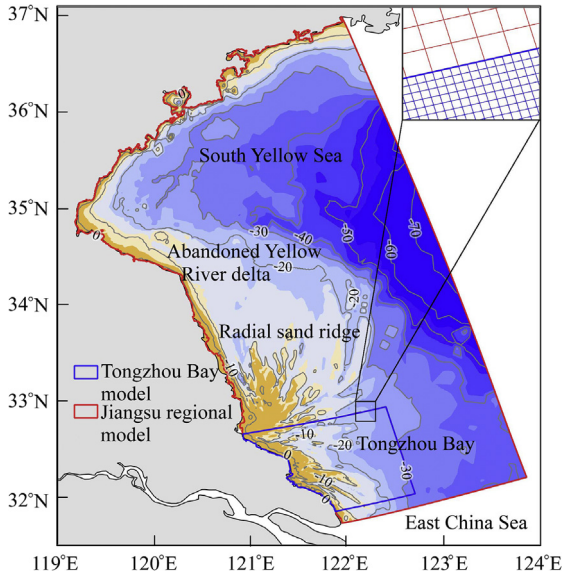

Fig. 2. Computational domains of Jiangsu regional model and Tongzhou Bay model (units of elevations: m).

Table 1
Ecotope feature classification.

Classification based on depth	Sub-classification based on dryfall period or depth	Ecotope name	
		High hydrodynamic ($v \geq 0.8$ m/s)	Low hydrodynamic ($v < 0.8$ m/s)
Supralittoral ($d > MHWN$)			Supralittoral (SL)
Littoral ($MLWS \leq d \leq MHWN$)	High-range ($P_D > 60\%$)	High-range littoral, high dynamic (HRL-HD)	High-range littoral, low dynamic (HRL-LD)
	Mid-range ($25\% \leq P_D \leq 60\%$)	Mid-range littoral, high dynamic (MRL-HD)	Mid-rrange littoral, low dynamic (MRL-LD)
	Low-range ($P_D < 25\%$)	Low-range littoral, high dynamic (LRL-HD)	Low-range littoral, low dynamic (LRL-LD)
Sublittoral ($d < MLWS$)	Shallow ($d < MLWS - 5$)	Shallow sublittoral, high dynamic (SSL-HD)	Shallow sublittoral, low dynamic (SSL-LD)
	Deep ($MLWS - 5 \leq d < MLWS$)	Deep sublittoral, high dynamic (DSL-HD)	Deep sublittoral, low dynamic (DSL-LD)

Note: d is the depth (m), P_D is the percentage of dryfall period in tidal cycle (%), and v is the velocity (m/s).

The JRM bathymetry was compiled from measurements through the radial sand ridge (RSR) system in 2006 and electronic navigational charts (Yao, 2016). This bathymetry was updated with higher-resolution bathymetric data of the Tongzhou Bay region, which was surveyed in October 2010.

The Reynolds-averaged Navier-Stokes equations for shallow water and the Boussinesq assumption were solved numerically on a staggered grid using the finite difference scheme for a two-dimensional (2D) depth-averaged environment. The JRM was driven by a series of astronomical tides at its two open boundaries (Fig. 2). These were derived from a set of 13 tidal harmonic components (i.e., M2, S2, K2, N2, K1, O1, P1, Q1, M4, MS4, MN4, MF, and MM) from a large-scale tidal wave model of the BYECS for a full morphological year time-series (Su et al., 2015).

2.4. Model performance evaluation

As the model was refined for the Tongzhou Bay region, revalidation was required. The model was validated through quantitative assessments of the calculated and measured values at several monitoring locations at Tongzhou Bay. These measurements were retrieved during spring and neap tidal conditions from February 22 to 23, 2012 (spring tide) and from February 29 to March 1, 2012 (neap tide) at 14 mooring stations and six tidal gauges in Tongzhou Bay (Fig. 1).

The quantitative validation was conducted through two statistical parameters. The first parameter was the Nash-Sutcliffe model efficiency coefficient (*NSE*) (Nash and Sutcliffe, 1970), which is as follows:

$$NSE = 1 - \frac{\sum (|m-p| - \Delta m)^2}{\sum (m-\overline{m})^2} \tag{1}$$

where m is the measured value, p is the value predicted or calculated by the model, $\overline{m}$ is the mean measured value, and Δm is the error in the measurements (van Rijn et al., 2003). The performance of the model was classified into the following classes: excellent ($NSE \geq 0.65$), very good ($0.5 \leq NSE < 0.65$), good ($0.2 \leq NSE < 0.5$), and poor ($NSE < 0.2$) (Allen et al., 2007; Henriksen et al., 2003).

The second parameter was the bias expressed in percentages (*PB*), which is as follows:

$$PB = \frac{\sum[(m-p) \pm \Delta m]}{\sum m} \times 100\% \tag{2}$$

where the numerator can either be $(m-p) - \Delta m$ (in the case of $m - p > 0$) or $(m-p) + \Delta m$ (in the case of $m - p < 0$). The value of $(m-p) \pm \Delta m$ is set to 0, if $(m - p) \pm \Delta m < 0$. The absolute values of *PB* were classified into four classes: excellent ($|PB| \leq 10\%$), very good ($10\% < |PB| \leq 20\%$), good ($20\% < |PB| \leq 40\%$), and poor ($|PB| > 40\%$) (Allen et al., 2007; Henriksen et al., 2003).

3. Results and discussion

3.1. Model performance

The statistical validation of the calculated water levels for both *NSE* and *PB* at the six tidal gauges (with M1 through M6 representing Sanshahong, Xiaomiaohong, Lengjiasha, Lüsi, Datang, and Yangkou stations, respectively) revealed an excellent performance of the model in predicting the water level, with an efficiency of $NSE > 0.65$ for all stations (Fig. 3). Similar results were obtained for the percentage bias, scoring good for the Xiaomiaohong and Datang stations and very good for all the other stations ($20\% < |PB| < 40\%$ and $|PB| < 20\%$, respectively).

The same statistical validation was performed for the current velocity and direction at the 14 mooring stations. Fig. 4 shows the *NSE* values for the current velocity and current direction. The model performed well in predicting the current velocities at most stations with an excellent score ($NSE > 0.65$). The current velocity at Station N6 (not shown in Fig. 4) diverged from this trend and showed a considerably poor performance ($NSE < 0.2$), which demonstrates that the observed mean is better than the model prediction. At this station, significantly low velocities were measured during ebb tides (with the peak flow less than 0.3 m/s), which is presumably due to inconsistencies in bathymetry or error in measurements. Stations N10, N12, and N13 showed a good performance ($0.2 < NSE < 0.5$). This is mainly due to the fact that these stations were situated in relatively shallow water and the velocity was less bidirectional compared to that at the other stations. The performance of the model in calculating the current direction ranges from very good to excellent

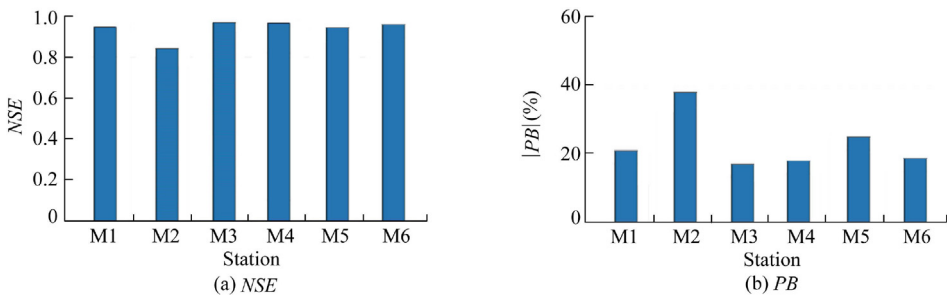

Fig. 3. Nash-Sutcliffe model efficiency coefficient and percentage bias for calculated water level at six tidal gauges.

($NSE > 0.5$) for most stations. Compared with the model performance in current velocity, the performance in current direction is poorer, due to the relatively large errors, even with a small difference in calculated and measured in current phase. Overall the model showed excellent to very good scores ($|PB| < 20\%$). As discussed earlier, the exception is the poor score in current velocities at the N6 station ($|PB| = 100\%$). These scores are similar to performance scores found by Yao (2016), signifying that the refinement did not cause less accuracy in predicting the hydrodynamics in Tongzhou Bay.

3.2. Ecotope map of Tongzhou Bay

The model output was subsequently converted into the ecotope map for Tongzhou Bay (Fig. 5), based on the definitions listed in Table 1. The Yaosha shoal was mainly classified as littoral ecotope, ranging from low-range littoral zone at the outer edges to high-range littoral and supralittoral zones close to the current seawall. This indicates that during mean high water springs (MHWS), nearly the whole extent of the Tongzhou Bay mudflats is inundated. The Lengjiasha shoal and other nearshore regions are within the shallow sublittoral zone, indicating constant inundation. The deeper sections of the Xiaomiaohong and Lengjiasha channels are mostly in the deep sublittoral zone. The hydrodynamic conditions roughly coincide with the overall elevations of the region, where the Yaosha and Lengjiasha shoals show low hydrodynamic conditions.

The bathymetry or elevation is the most influential factor in ecotope classification, as it also governs the hydrodynamics and dryfall periods. The created ecotope map showed that the hydrodynamic classification followed the elevation quite closely. As the elevation changes rapidly from deep channels to shallow flats with steep edges, a similar shift can be observed between low and high hydrodynamic conditions. This suggests that the hydrodynamic classification and chosen class bound are rather robust. As the more dominant elevation changes diminish within the littoral zone, the sub-classification based on the dryfall period becomes more sensitive to the set class bounds. Specific validation of these intertidal dryfall periods, such as specific field measurements, is therefore required.

The retrieved ecotope map was subsequently overlaid with the 50%, 90%, and 95% home ranges of the two shorebird species (Fig. 6), with the degree of overlap shown in Table 2. Both species mainly occurred in the mid-range (30%−40%) and low-range (18%−19%) littoral zones. This is in line with the general knowledge of habitat preferences of the two shorebird species. Both species specialize in foraging on benthic organisms in intertidal mudflats. GK is a shellfish specialist (Zhang et al., 2019), while BTG is a generalist (Duijns et al., 2013). With its long bill, BTG can forage not only on shellfish, but also on worms deep in the sediment. Moreover, BTG is characterized as a *tide-follower*, moving up and down the mudflat following the tideline (Piersma et al., 2017). Hence, we can conclude that the mid-range and low-range littoral zones, which overlap with 49%−60% of their 90% home ranges, represent the most used habitat conditions for both BTG and GK.

3.3. Impact of reclamation activities on ecotope distribution

The current reclamation activities on Tongzhou Bay (Fig. 5) cover approximately 35.9 km^2, including the U-shaped

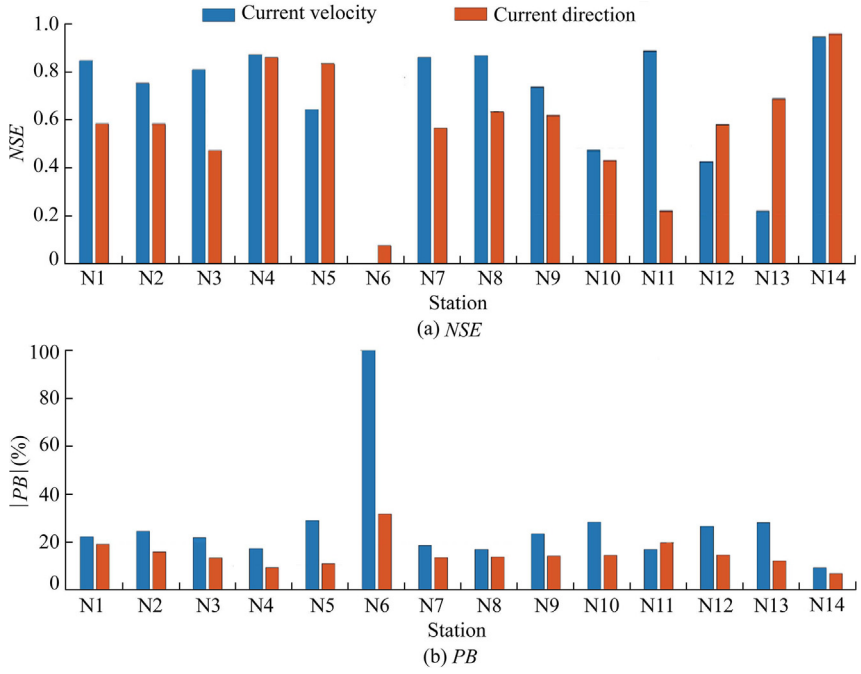

Fig. 4. Nash-Sutcliffe model efficiency coefficient and percentage bias for calculated current velocity and direction at 14 mooring stations.

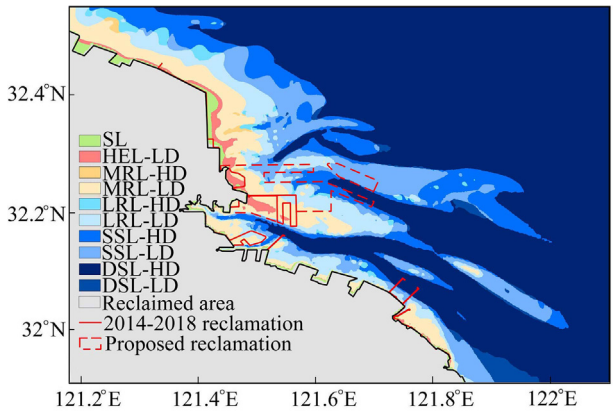

Fig. 5. Ecotope map of Tongzhou Bay as of 2012.

basin at Yaosha, covering 12.12 km^2, and are similar to the work described in Huang and Liu (2017). The proposed port development expands these existing reclamations and covers approximately 126 km^2, resulting in a total reclaimed area of 161.9 km^2 to be completed by 2035.

The impact of the current and proposed reclamations on the ecosystem was further assessed by calculating the area of each ecotope lost due to the current and proposed reclamation configurations, as a fraction of the extent of the original ecotope map (Fig. 5). Results are shown in Fig. 7. The reclamation from 2014 to 2018 was carried out at the upper reaches of the tidal flats, which are classified as supralittoral, high-range littoral, and mid-range littoral zones in low hydrodynamic conditions (5%, 15%, and 9%, respectively). The proposed reclamation for 2018−2035 expands within these ecotopes. The port expansion will occur in the high-range, mid-range, and low-range littoral zones (27%, 39%, and 34%, respectively). The combined current and proposed reclamations would lead to loss of high-range (42%), mid-range (48%), and low-range (38%) littoral zones (low and high hydrodynamic conditions combined). This corresponds to 44%−45% loss of the most important ecotopes (mid-range and low-range littoral zones) for BTG and GK.

3.4. Future opportunities

The current assessment of the impact of the ongoing reclamation on ecotope occurrence and potential habitat gives more insight into the potential risk that is involved with large-scale reclamation in coastal habitats, and the vital ecosystem services they provide. However, this assessment tool can also be used to determine the input value during the design stage. The composition of an ecotope map can provide additional ecosystem-based information to govern the design of coastal interventions.

In order to increase the accuracy of the created ecotope map, it is recommended to increase the set of abiotic parameters and data sources for the ecotope classification and subsequent validation. Including distributional data of more species of different ecosystem functions and investigating how their spatial distributions change throughout the tidal cycle (e.g., Chan et al., 2019a), will enhance the insight into the value of certain ecotopes and the vital functions they provide within the coastal ecosystem.

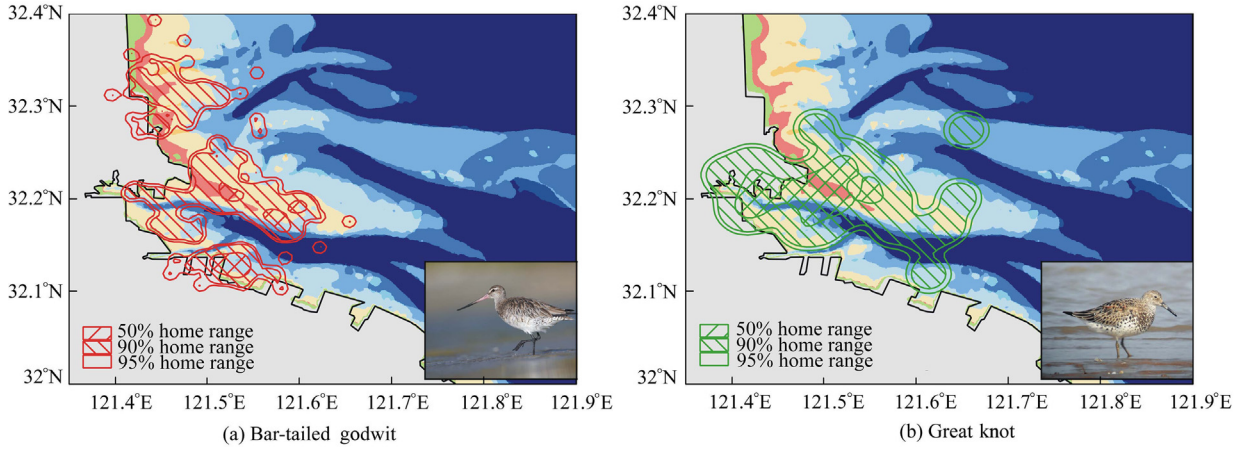

Fig. 6. Ecotope map of Tongzhou Bay and home range of bar-tailed godwit and great knot on southern Jiangsu coast from April 2015 to September 2017 (refer to Fig. 5 for ecotope color).

Table 2
Degree of overlap of ecotopes corresponding with 90% home range of bar-tailed godwit and great knot.

Shorebird species	Degree of overlap (%)										
	Reclaimed	SL	HRL-LD	MRL-HD	MRL-LD	LRL-HD	LRL-LD	SSL-HD	SSL-LD	DSL-HD	DSL-LD
Bar-tailed godwit	9	5	7	1	40	4	15	15	3	1	0
Great knot	20	7	4	0	30	1	18	7	8	15	0

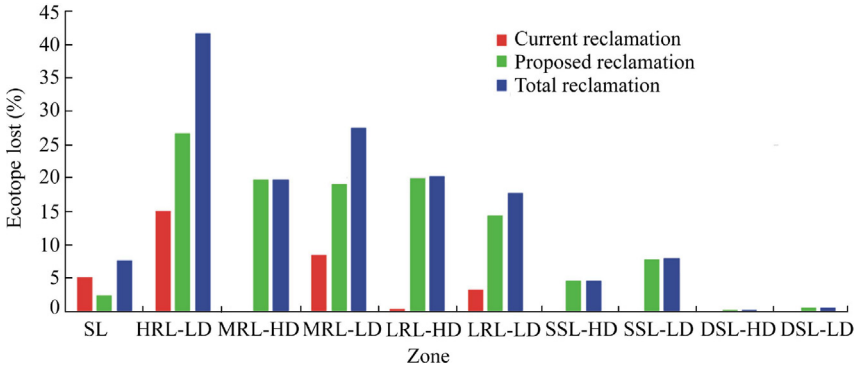

Fig. 7. Percentage of lost ecotope area with respect to total extent of ecotope map due to current, proposed, and total reclamations.

Reclamation has a severe effect on local hydrodynamics and transport agents and therefore the occurrence of ecotopes. In the classification process, the water depth is the most hierarchical parameter. Subsequent ecotope development could be investigated through morphodynamic modeling, which should be the next step in assessing the impact of reclamation on intertidal habitat.

4. Conclusions

In this study, an ecotope map was constructed to assess the current and proposed reclamation activities on Tongzhou Bay. The following conclusions were drawn:

(1) Spatial abiotic data (salinity and bathymetry) and hydrodynamic model output (dryfall period and flow velocity) were used to classify a set of 11 ecotopes, as bases for the ecotope map of Tongzhou Bay for 2012. This map was validated with satellite-tracked spatial data on two main threatened shorebird species (BTG and GK) occurring in this area. This showed a strong correspondence with mid- and low-range littoral zones, suggesting that these ecotopes represent the preferred habitat conditions for these species. This was further confirmed with previous knowledge on habitat preferences of these two species.

(2) The reclamation activities of 2014−2018 and proposed reclamation for 2018−2035, largely take place at the nearshore shoals (e.g., Yaosha and Lengjiasha). The reclamation activities of 2014−2018 were carried out at the center of Yaosha shoal, reclaiming supralittoral or high-range littoral, and mid-range littoral zones in low hydrodynamic conditions (5%, 15%, and 9% of the retrieved ecotope map extent, respectively). The proposed reclamation for 2018−2035 will expand on the current reclamation and mostly cover the high-range, mid-range, and low-range littoral areas (27%, 39%, and 34% of the current ecotope map extent, respectively). The total of the proposed and current reclamations would cover high-range littoral (42%), mid-range littoral (48%), and low-range littoral (38%) areas, corresponding to a 44%−45% loss of the most important ecotopes (mid-range and low-range littoral zones) for BTG and GK.

(3) The use of ecotope maps as a basis for the quantification of the environmental impact of marine infrastructure over time enables early inclusion of habitat requirements in the design process of coastal works.

Acknowledgements

The authors would like to acknowledge Prof. Chang-kuan Zhang, Dr. Zeng Zhou, and Dr. Ao Chu at Hohai University, who contributed importantly to the data analysis and model development. We thank many volunteers who helped in the expeditions to deploy satellite transmitters onto shorebirds in Australia, including Chris Hassell who organized these expeditions, and Lee Tibbitts who curated the satellite tracking data. The satellite tracking was supported by the Spinoza Premium 2014 awarded by the Netherlands Organization for Scientific Research (NWO) to Theunis Piersma, by the MAVA Foundation, Switzerland, with additional support from WWF-Netherlands and BirdLife Netherlands. Ying-chi Chan was supported by the Ubbo Emmius Fund of the University of Groningen and by the Spinoza Premium 2014 to Theunis Piersma. Finally, the financial support by the Lamminga Foundation to Jos R. M. Muller is also greatly acknowledged.

References

Allen, J.I., Somerfield, P.J., Gilbert, F.J., 2007. Quantifying uncertainty in high-resolution coupled hydrodynamic-ecosystem models. J. Mar. Syst. 64, 3−14. https://doi.org/10.1016/j.jmarsys.2006.02.010.

Australian Government, 2019. Species profile and threats database. http://www.environment.gov.au/cgi-bin/sprat/public/sprat.pl [Retrieved July 28, 2019].

Baptist, M.J., van der Wal, J.T., de Groot, A.V., Ysebaert, T.J.W., 2016. Ecotopenkaart Waddenzee Volgens de ZES.1 Typologie (No. Wageningen Marine Research Rapport C103/16). Wageningen University & Research, Den Helder (in Dutch).

Baptist, M.J., van der Wal, J.T., Folmer, E.O., Gräwe, U., Elschot, K., 2019. An ecotope map of the trilateral Wadden Sea. J. Sea Res. 152, 101761. https://doi.org/10.1016/j.seares.2019.05.003.

Battley, P.F., Warnock, N., Tibbitts, T.L., Gill, R.E., Piersma, T., Hassell, C.J., Douglas, D.C., Mulcahy, D.M., Gartell, B.D., Schuckard, R., et al., 2012. Contrasting extreme long-distance migration patterns in bar-tailed godwits *Limosa lapponica*. J. Avian Biol. 43(1), 21−32. https://doi.org/10.1111/j.1600-048X.2011.05473.x.

Bouma, H., de Jong, D.J., Twisk, F., Wolfstein, K., 2005. Zoute wateren ecotopen stelsel (ZES.1). Voor Het in Kaart Brengen van Het Potentiële Voorkomen van Levensgemeenschappen in Zoute en Brakke Rijkswateren. (No. Rapport RIKZ/2005.024). Ministerie van Verkeer en Waterstaat, Middelburg (in Dutch).

CCCC Third Harbor Consultants Co., Ltd., 2012. Hydrological Analysis Report of Tongzhou Qianwan Planning. CCCC Third Harbor Consultants Co., Ltd., Shanghai (in Chinese).

Chan, Y.-C., Peng, H.-B., Han, Y.X., Chung, S.S.W., Li, J., Zhang, L., Piersma, T., 2019a. Conserving unprotected important coastal habitats in the Yellow Sea: Shorebird occurrence, distribution and food resources at Lianyungang. Global Ecology and Conservation 20, e00724. https://doi.org/10.1016/j.gecco.2019.e00724.

Chan, Y.-C., Tibbitts, T.L., Lok, T., Hassell, C.J., Peng, H.-B., Ma, Z., Zhang, Z., Piersma, T., 2019b. Filling knowledge gaps in a threatened shorebird flyway through satellite tracking. J. Appl. Ecol. 56(10), 2305−2315. https://doi.org/10.1111/1365-2664.13474.

Duijns, S., Hidayati, N.A., Piersma, T., 2013. Bar-tailed godwits *Limosa l. lapponica* eat polychaete worms wherever they winter in Europe. Hous. Theor. Soc. 60(4), 509−517. https://doi.org/10.1080/00063657.2013.836153.

Henriksen, H.J., Troldborg, L., Nyegaard, P., Sonnenborg, T.O., Refsgaard, J.C., Madsen, B., 2003. Methodology for construction, calibration and validation of a national hydrological model for Denmark. J. Hydrol. 280(1−4), 52−71. https://doi.org/10.1016/S0022-1694(03)00186-0.

Huang, L., Liu, B., 2017. Entrance layout and sedimentation reduction measures of the first and second basin in Tongzhou Bay Port. China Harb. Eng. 37, 29−34 (in Chinese). https://doi.org/10.7640/zggwjs201704008.

Kang, Y.Y., Ding, X.R., Zhang, C.K., 2015. Maximum tidal range analysis of radial sand ridges in the southern Yellow Sea. In. J. Geo-Marine Sci. 44, 971−976.

Lesser, G.R., Roelvink, J.A., van Kester, J.A.T.M., Stelling, G.S., 2004. Development and validation of a three-dimensional morphological model. Coast. Eng. 51(8−9), 883−915. https://doi.org/10.1016/j.coastaleng.2004.07.014.

Ma, Z.J., Melville, D.S., Liu, J.G., Chen, Y., Yang, H.Y., Ren, W.W., Zhang, Z.W., Piersma, T., Li, B., 2014. Rethinking China's new great wall: Massive seawall construction in coastal wetlands threatens biodiversity. Science 346(6212), 912−914. https://doi.org/10.1126/science.1257258.

Murray, N.J., Clemens, R.S., Phinn, S.R., Possingham, H.P., Fuller, R.A., 2014. Tracking the rapid loss of tidal wetlands in the Yellow Sea. Front. Ecol. Environ. 12(5), 267−272. https://doi.org/10.1890/130260.

Murray, N.J., Ma, Z.J., Fuller, R.A., 2015. Tidal flats of the Yellow Sea: A review of ecosystem status and anthropogenic threats. Austral Ecol. 40(4), 472−481. https://doi.org/10.1111/aec.12211.

Nantong Leju Network, 2019. General Plan of the Tongzhou Bay Zone in Jiangsu Province (2018−2035). https://nt.leju.com/news/2019-05-09/07456532037622683202027.shtml [Retrieved July 30, 2019].

Nash, J.E., Sutcliffe, J.V., 1970. River flow forecasting through conceptual models part I: A discussion of principles. J. Hydrol. 10(3), 282−290. https://doi.org/10.1016/0022-1694(70)90255-6.

Peng, H.-B., Anderson, G.Q.A., Chang, Q., Choi, C.-Y., Chowdhury, S.U., Clark, N.A., Gan, X., Hearn, R.D., Li, J., Lappo, E.G., et al., 2017. The intertidal wetlands of southern Jiangsu Province, China: Globally important for Spoon-billed Sandpipers and other threatened waterbirds, but facing multiple serious threats. Bird. Conserv. Int. 27(3), 305−322. https://doi.org/10.1017/S0959270917000223.

Piersma, T., Lok, T., Chen, Y., Hassell, C.J., Yang, H.-Y., Boyle, A., Slaymaker, M., Chan, Y.-C., Melville, D.S., Zhang, Z.-W., et al., 2016. Simultaneous declines in summer survival of three shorebird species signals a flyway at risk. J. Appl. Ecol. 53(2), 479−490. https://doi.org/10.1111/1365-2664.12582.

Piersma, T., Chan, Y.-C., Mu, T., Hassell, C.J., David, S.D.S., Peng, H.-B., Ma, Z., Zhang, Z., Wilcove, D.S., 2017. Loss of habitat leads to loss of birds: Reflections on the Jiangsu, China, coastal development plans. Wader Study 124(2), 93−98. https://doi.org/10.18194/ws.00077.

Su, M., Yao, P., Wang, Z.B., Zhang, C.K., Stive, M.J.F., 2015. Tidal wave propagation in the Yellow Sea. Coast Eng. J. 57(3), 1550008. https://doi.org/10.1142/S0578563415500084.

Su, M., 2016. Progradation and Erosion of a Fine-Grained, Tidally Dominated Delta: A Case Study of the Jiangsu Coast. Ph. D. Dissertation. Delft University of Technology, Delft.

Tao, J., Zhang, C.K., Yao, J., 2011. Effect of large-scale reclamation of tidal flats on tides and tidal currents in offshore areas of Jiangsu Province. J. Hohai Uni. (Nat. Sci.) 39(2), 225−230 (in Chinese). https://doi.org/10.3876/j.issn.1000-1980.2011.02.020.

Tian, B., Wu, W.T., Yang, Z.Q., Zhou, Y.X., 2016. Drivers, trends, and potential impacts of long-term coastal reclamation in China from 1985 to 2010. Estuarine. Coast. Shelf Sci. 170, 83−90. https://doi.org/10.1016/j.ecss.2016.01.006.

van Rijn, L.C., Walstra, D.J.R., Grasmeijer, B., Sutherland, J., Pan, S., Sierra, J.P., 2003. The predictability of cross-shore bed evolution of sandy beaches at the time scale of storms and seasons using process-based profile models. Coast. Eng. 47(3), 295−327. https://doi.org/10.1016/S0378-3839(02)00120-5.

Wang, F., Wall, G., 2010. Mudflat development in Jiangsu Province, China: Practices and experiences. Ocean Coast Manag. 53(11), 691−699. https://doi.org/10.1016/j.ocecoaman.2010.10.004.

Wang, Y.P., Gao, S., Jia, J., Thompson, C.E.L., Gao, J., Yang, Y., 2012. Sediment transport over an accretional intertidal flat with influences of reclamation, Jiangsu coast, China. Mar. Geol. 291−294, 147−161. https://doi.org/10.1016/j.margeo.2011.01.004.

Wu, G.X., Li, H.J., Liang, B.C., Shi, F.Y., Kirby, J.T., Mieras, R., 2017. Subgrid modeling of salt marsh hydrodynamics with effects of vegetation and vegetation zonation. Earth Surf. Process. Landforms 42(12), 1755−1768. https://doi.org/10.1002/esp.4121.

Xing, F., Wang, Y.P., Wang, H.V., 2012. Tidal hydrodynamics and fine-grained sediment transport on the radial sand ridge system in the southern Yellow Sea. Mar. Geol. 291−294, 192−210. https://doi.org/10.1016/j.margeo.2011.06.006.

Xu, F., Tao, J., Zhou, Z., Coco, G., Zhang, C., 2016. Mechanisms underlying the regional morphological differences between the northern and southern radial sand ridges along the Jiangsu Coast, China. Mar. Geol. 371, 1−17. https://doi.org/10.1016/j.margeo.2015.10.019.

Yao, P., 2016. Tidal and Sediment Dynamics in a Fine-Grained Coastal Region: A Case Study of the Jiangsu Coast. Ph. D. Dissertation. Delft University of Technology, Delft.

Zhang, C.K., Chen, J., 2011. Master plan of tidal flat reclamation along Jiangsu coastal zone. In: Proceedings of 6th International Conference on Asian and Pacific Coasts. Weizmann Institute of Science, Hong Kong, pp. 139−146.

Zhang, C., Zheng, J., Dong, X., Cao, K., Zhang, J., 2013. Morphodynamic response of Xiaomiaohong tidal channel to a coastal reclamation project in Jiangsu Coast, China. J. Coast Res. 65(s1), 630−635. https://doi.org/10.2112/SI65-107.1.

Zhang, S.-D., Ma, Z., Choi, C.-Y., Peng, H.-B., Melville, D.S., Zhao, T.-T., Bai, Q.-Q., Liu, W.-L., Chan, Y.-C., van Gils, J.A., et al., 2019. Morphological and digestive adjustments buffer performance: How staging shorebirds cope with severe food declines. Ecol. Evol. 9(7), 3868−3878. https://doi.org/10.1002/ece3.5013.